

LOCALIZED INDUCTION HEATING BASED CONTROL OF REACTIVE RESIN FLOW IN A VARTM PROCESS

R.J. Johnson¹ and R. Pitchumani^{1,2}

¹ *Advanced Materials and Technologies Laboratory, Department of Mechanical Engineering, Storrs, CT 06269-3139 <http://www.engr.uconn.edu/amtl>; presently with: ASML, Wilton, CT*

² *Corresponding Author's Email: pitchu@engr.uconn.edu*

SUMMARY: One particular challenge in liquid molding, in general, is the filling of a fibrous preform-laden mold with catalyzed resin. The permeability variability causes non uniformity in the fill patterns, and often leads to entrapped voids and dry spots in the product. The goal of this work is to devise an active control strategy that overcomes this problem. A novel scheme based on the concept of locally reducing resin viscosity in real time, in areas of low permeability using induction heating, is explored by considering the VARTM process. A consequence of localized heating of reacting resin is an accelerated cure reaction that irreversibly increases resin viscosity. A balance between the competing sources of viscosity changes form the basis for a model-based control of localized heating. Numerical and experimental results using the flow control scheme are presented and show successful mold filling without entrapment of dry spots.

KEYWORDS: induction heating, Vacuum Assisted Resin Transfer Molding (VARTM), active control, permeability, resin cure, rheology

INTRODUCTION

In the vacuum assisted resin transfer molding (VARTM) process, fibrous preform material is sandwiched between a single-sided hard mold half and a vacuum bag; vacuum is drawn on the system that compacts the preform and draws reactive resin from the mold inlet ports, through the porous preform, to the vacuum vents. Defects are often introduced during the filling stage when the flow does not fully impregnate a region of the preform. The goal of the present work is to demonstrate application of a localized-heating-based active flow control methodology for mold filling with a catalyzed resin system in a VARTM process. Since the rheology of the resin system is such that the viscosity decreases with temperature but increases with the degree of cure, the active control scheme must balance these competing effects on viscosity introduced by the heating. Furthermore, from a processing viewpoint, it is important to ensure that the resin does not prematurely gel as a result of the heating during the filling process. This paper describes an active control scheme based on induction heating that achieves these multiple objectives.

ACTIVE CONTROL

Controller Architecture

The goal of the active control scheme is to determine, in real time, the target position of an induction coil and the power (voltage) supplied to it so as to (a) steer the flow to follow a uniform trajectory, (b) minimize the fill time, and (c) keep the degree of cross linking at the end of fill to be less than a specified critical value. The active control architecture designed to meet these objectives is shown schematically in Fig. 1 as described in this section. The controller consists of two main modules—a coil location estimator and coil voltage estimator—that interface with the prototype VARTM process and a real time flow sensor.

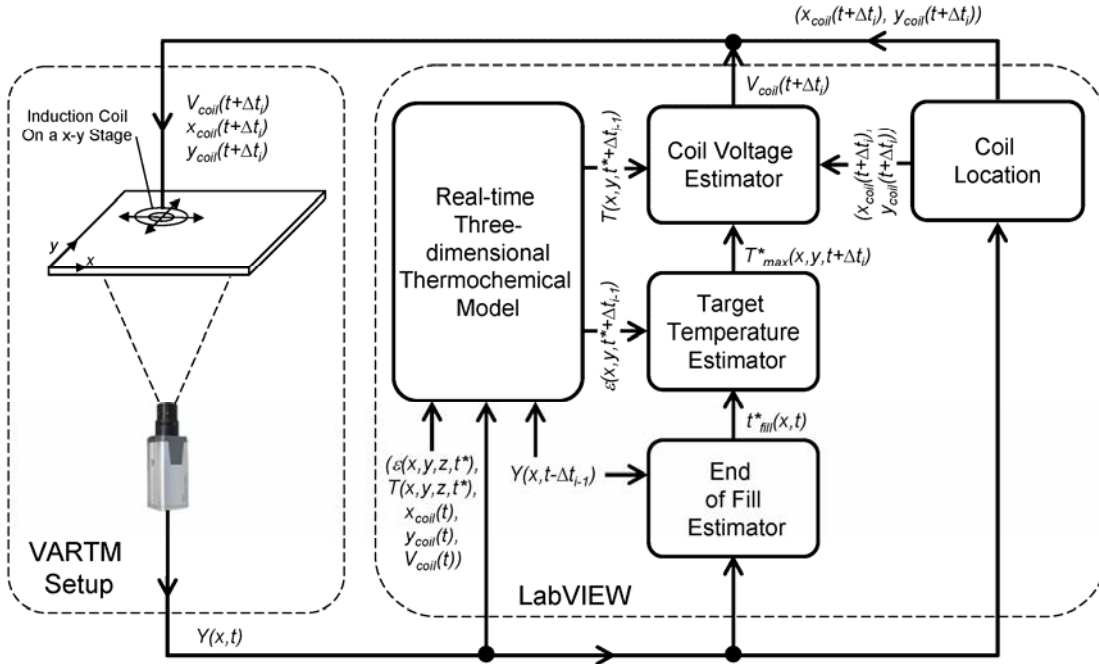


Fig. 1 Schematic diagram of the active controller architecture for active control of reactive resin flow in a VARTM process.

At any time instant, t , the flow front location, $Y(x,t)$, is sensed by the camera and fed to the controller. The coil location estimator uses this information to determine the target coil position, $[x_{coil}(t + \Delta t_i), y_{coil}(t + \Delta t_i)]$ for the next time step, such that the center of the coil is in line with the largest flow lag in the x -direction and the heated area underneath the coil is just behind the flow front in the y -direction. This strategy for coil positioning was shown to be most effective in locally reducing the viscosity and improving flow uniformity and flow rate in a previous study [1]. The coil location information is fed forward to the VARTM setup for the positioning of the coil at the time $t + \Delta t_i$, and is also passed to the coil voltage estimator module of the controller.

The voltage estimation is made so as to minimize the fill time by maximizing the heating and the viscosity reduction, while ensuring that the degree of cure in the resin at the end of fill is within a specified value, ε_L . To this end, the procedure consists of (a) estimating the fill time, t_{fill}^* , based

on the current conditions of the flow, (b) estimating the maximum isothermal temperature, T_{\max}^* , that would lead to the degree of cure at the end of the estimated fill time to be within the critical value, ε_L , and (c) relating the maximum isothermal temperature, T_{\max}^* , to the voltage of the induction coil, $V_{coil}(t + \Delta t)$, that is passed to the induction heating system. This sequence of estimation is illustrated in Fig. 1, as described below.

The fill time is estimated by invoking the idealized one-dimensional form of Darcy's law [2, 3] applied to linear length-wise flow segments at several locations across the mold width, to obtain a distribution of estimated fill times, $t_{fill}^*(x, t)$, for each of the flow segments. The maximum isothermal temperature estimate is obtained such that the degree of cure in the resin at the time the flow front reaches the end of the mold, i.e., at the estimated fill time Δt_{fill}^* , is less than the constraint value ε_L . The kinetics of the autocatalytic cure reaction for the resin system chosen in this study is governed by an Arrhenius-type equation of the form:

$$\frac{d\varepsilon}{dt} = \left(K_0 e^{-E/RT} \varepsilon^m \right) (1 - \varepsilon)^n \quad (1)$$

where K_0 is the frequency factor, E is the activation energy, m and n are empirical exponents whose values are such that $m + n = 2$ [4–7]. Advection terms have been neglected to obtain a conservative estimate of maximum isothermal temperature. Separating variables in Eqn. 1 and integrating from the current degree of cure, $\bar{\varepsilon}(x, y, t_{fill}^*)$, to the maximum degree of cure constraint at the estimated fill time, $\bar{\varepsilon}(x, y, t_{fill}^*) = \varepsilon_L$, and rearranging the resulting expression, the maximum isothermal temperature, $T_{\max}^*(x, y, t + \Delta t_{i-1})$, is obtained as

$$T_{\max}^*(x, y, t + \Delta t_{i-1}) = \frac{E}{R \ln \left[K_0 \left(t_{fill}^*(x, y, t) - t \right) / \int_{\bar{\varepsilon}(x, y, t)}^{\varepsilon_L} \frac{d\varepsilon}{\varepsilon^m (1 - \varepsilon)^{2-m}} \right]} \quad (2)$$

where $\bar{\varepsilon}$ denotes the thickness-averaged degree of cure profile, which is obtained from an online thermochemical numerical simulation model described in below.

The induction coil voltage at the next control interval, $V_{coil}(t + \Delta t_i)$, is determined using a simplified lumped capacitance description of energy transport of the form:

$$\rho c \frac{\partial T(x, y, t)}{\partial t} = \frac{-c_f h}{d} (T(x, y, t) - T_\infty) + q'''(x, y, t) \quad (3)$$

where the left hand side is the energy accumulation rate given by a balance between the volumetric heat generation due to induction heating, $q'''(x, y, t)$, that is dependent on the induction voltage [1,8] and the energy loss by convection to the ambient [9]. In the above equation h is the convection heat transfer coefficient, d is the molded part thickness, $T(x, y, t)$ is the resin saturated preform temperature obtained from the numerical three-dimensional thermochemical model being run in real-time, corresponding to the coil voltage $V(x, y, t)$, and T_∞ is the ambient temperature. The coefficient c_f is a factor that compensates for the following simplifying assumptions: uniform temperature through the thickness, negligible conduction in every direction, and negligible advection. Eqn. 3 yields a two-dimensional solution for the temperature distribution, $T(x, y, t + \Delta t_{i-1})$, in the mold; setting this temperature to be

$T_{\max}^*(x, y, t + \Delta t_{i-1})$, the desired maximum isothermal temperature is calculated using Eqn. 2. The temperature solution is used to obtain the required volumetric heat generation, $q'''(x, y, t + \Delta t_{i-1})$, to achieve the maximum isothermal temperature, $T_{\max}^*(x, y, t + \Delta t_{i-1})$, in one control interval, Δt_{i-1} which is then correlated to the coil voltage $V_{coil}(t)$. The thermochemical model referenced above is used to simulate the three dimensional cure and temperature distributions within the mold in real time. The model is used for the following purposes: (a) provide a substitute for the experimental process and allow for large scale parametric studies to be performed by simulation; and (b) to provide temperature and cure distribution estimates in real-time as part of the active control system. Details of the model are not provided here in the interest of brevity, but may be found in ref. [10].

Controller Implementation

The active flow control architecture was implemented on a lab-scale setup, shown in Fig. 2, consisting of a single-sided solid mold, a resin source and trap, a venturi pump to create vacuum pressures. Preform material is placed in the mold between the inlet and vent and the mold is sealed with a vacuum bag and Tacky-Tape (Schnee-Morehead, Inc., Texas).

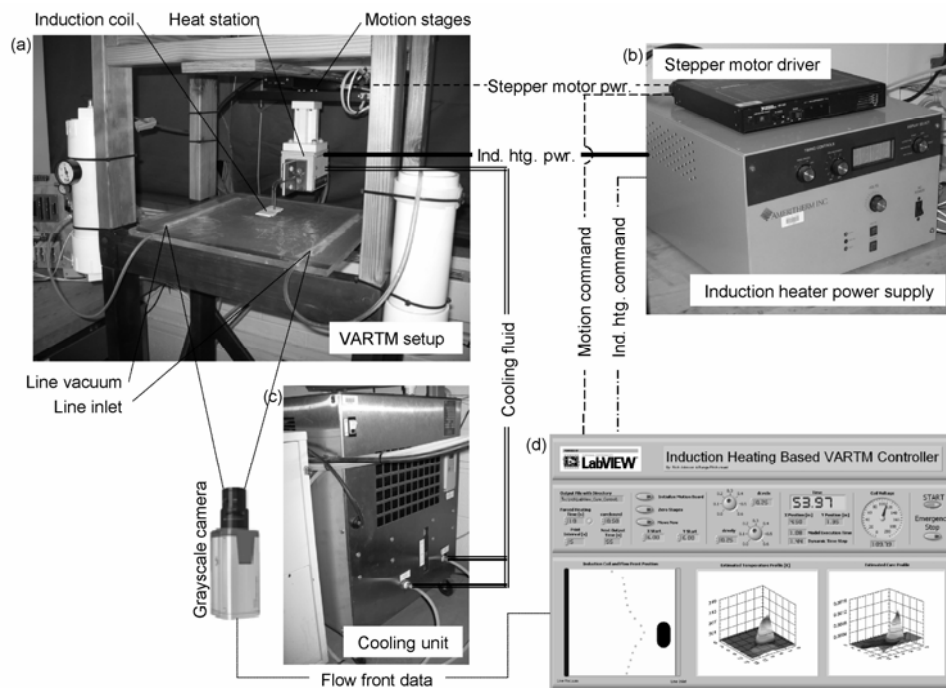


Fig. 2 Schematic of a VARTM setup with the capability for localized heating and active control.

The VARTM system is supplemented by induction heating based active flow control hardware. The induction heating system consists of a power supply, heating station with pancake style induction coil and cooling unit. High voltage (up to 200 V), high frequency (211 kHz) energy is delivered to the induction coil by the power supply, through the heating station. The current passing through the induction coil generates a magnetic field that induces an electric current through a conductive susceptor embedded in the preform; the resistance of the susceptor material

leads to Ohmic heating. In order to provide localized induction heating on demand, the coil is mounted on a two-axis motion stage system so that the coil can be positioned on a plane at a fixed distance above the top surface of the mold.

The control architecture (Fig. 1) described above was implemented in LabVIEW with the three-dimensional (3D) thermochemical models running in MATLAB scripts, which provided the induction coil voltage and the coil position in real-time with the process to the LabVIEW based induction heating controller and motion controller. The flow front location in real-time was captured using a machine vision system. A user interface was also designed and implemented in Labview to provide the target inputs to the controller as well as for monitoring the progress of the various aspects of the controller. A screen shot of this user interface is shown in Fig. 2d.

RESULTS AND DISCUSSION

Numerical and experimental studies were conducted on the model-based active control methodology discussed in the previous sections to systematically investigate the performance of the control logic. One example case and will be shown here. The numerical case simulates the filling of a $12\text{ in} \times 12\text{ in}$ mold with the rightmost quadrant adjacent to the line inlet filled with relatively low permeability preform as depicted in the image at the top right of Fig. 3a.

While ensuring that the active control scheme does not lead to premature resin gelation is one of the considerations, the primary goal of the active control is to improve flow uniformity during fill. To this end, a flow front uniformity measure was defined as the root-mean-squared error, e_{RMS} , between the actual flow front and an ideal target flow front at each instant during the fill. The time variation of the root-mean-squared error, e_{RMS} , is plotted in Fig. 3a for six different constraints on the maximum ending cure. The error initially increases due to the non-uniform flow front caused by the heterogeneous preform layup. Once the active control is initiated around 100 seconds, the error is reduced for all controlled cases ($\varepsilon_L > 0.0$) compared to the uncontrolled case ($\varepsilon_L = 0.0$). Increases in ε_L lead to more uniform flow fronts shown by the lower e_{RMS} values, and reductions in the complete mold fill time, t_{fill} . An integral of the time trace of the RMS error, e_{RMS} , provides a quantitative measure of the overall uniformity of the entire filling process, this integral normalized by the fill time of the uncontrolled case ($\varepsilon_L = 0.0$) is denoted as the normalized cumulative RMS error, e_{RMS}^* in the following discussion. In addition to the fill time, t_{fill} , and the normalized cumulative RMS error, e_{RMS}^* , it is also of interest to determine the time when the first part of the flow reaches the line vent, t_{fill}^* . This time is indicated by the filled circle on the line corresponding to $\varepsilon_L = 0.0$ in Fig. 6(b) as an example. For time beyond t_{fill}^* , the resin continues to flow through the filled regions into the vent leading to resin wastage, while the unsaturated preform regions are saturated by the resin. Thus, the ratio t_{fill}/t_{fill}^* is a measure of resin wastage, such that $t_{fill}/t_{fill}^* = 1$ is the ideal target corresponding to no resin waste.

The normalized cumulative RMS error, e_{RMS}^* , is plotted in Fig. 3b for three permeability sets Permeability Set 1: permeability ratio = 2 with overall relatively low permeability, Permeability

Set 2: permeability ratio = 10, and Permeability Set 3: permeability ratio = 2 with overall relatively high permeability. In general, an increase in the constraint value, ε_L , leads to reduced normalized cumulative RMS error. A relaxed constraint (higher ε_L) allows for increased local heating of the flowing resin without violation of the constraint, thereby enabling improved uniformity of flow front profile over the duration of the mold fill.

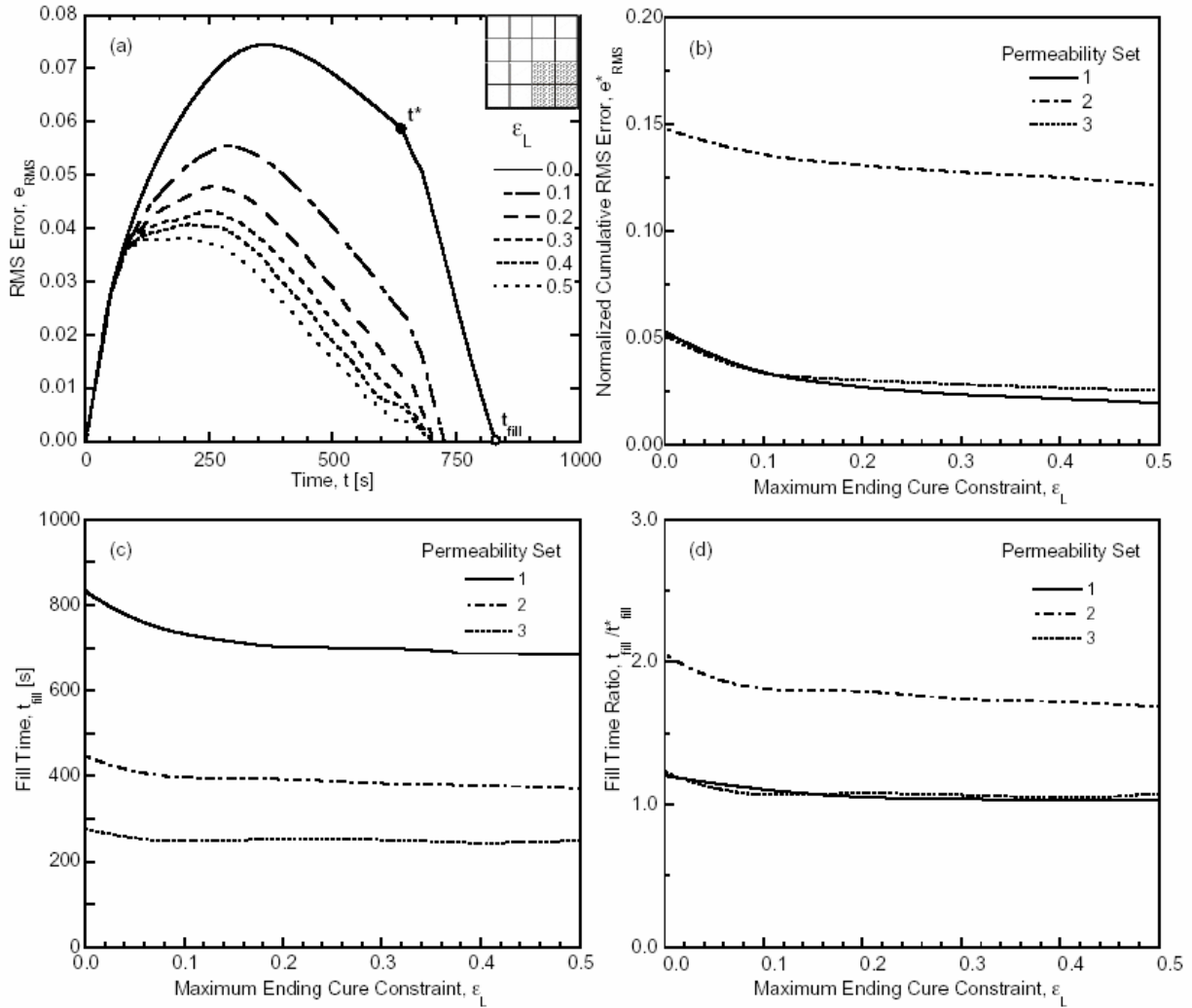


Fig. 3 (a) Time trace of the RMS error, and Permeability Set 1; (b) normalized cumulative RMS error, e_{RMS}^* , variation with the maximum ending cure constraint; (c) fill time, t_{fill} , variation with the maximum end of cure constraint; (d) fill time ratio, t_{fill}/t_{fill}^* , variation with the maximum end of cure constraint, ε_L .

Fig. 3c shows the fill times, t_{fill} , for the same cases shown in Fig. 3b. Fill time reductions are seen for larger ε_L , especially for Permeability Sets 1 and 2 which include very low permeability regions. Overall, Fig. 3c indicates that the active control is effectively limiting the degree of cure of the flowing resin such that the reduction in viscosity from locally elevated temperature outweighs the increases in viscosity due to the irreversible cure reaction and the overall fill times

are reduced. The fill time ratio, t_{fill}/t_{fill}^* , is plotted in Fig. 3d where a reduction in fill time ratio with increasing ε_L signifies that the active control is reducing the amount of wasted resin.

The control logic presented in above was implemented in Labview with the experimental setup pictured in Fig. 2. Results for a preform layup with a central low permeability patch (permeability ratio > 10) are shown in Fig. 4. For each run, a non dimensional measure of the flow uniformity, e , was defined as the area between the flow front and an ideal uniform flow front divided by the total surface area of the mold. Fig. 4 shows the variation of the non dimensional error with time during (a) an uncontrolled mold fill, (b) an actively controlled mold fill. Also shown in Fig. 4 are image captures of the flow front geometry taken at various times during each experiment.

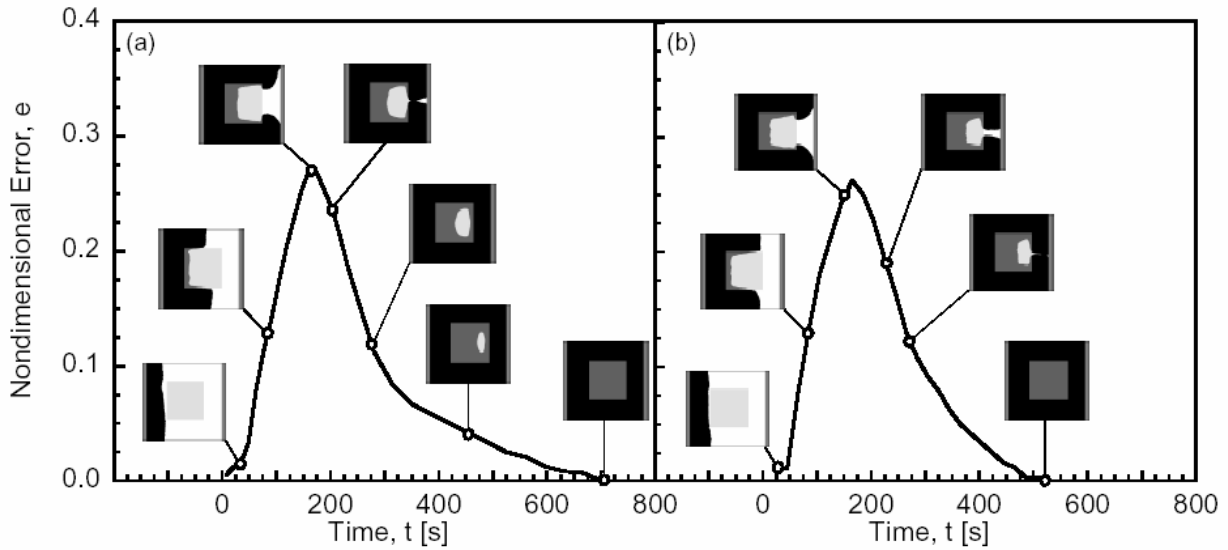


Fig. 4 Time traces of non dimensional error, e , for the two following cases:
 (a) uncontrolled mold fill, (b) actively controlled mold fill.

In the uncontrolled case [Fig. 4a] the error grows rapidly as the flow enters the low permeability region, reaches a peak and starts to decline just after the flow begins to reach the vent at $t_{fill}^* = 150$ s. The error reduces slowly as the flow entraps a void, but over time, as resin continues to flow into the vent, the void is eliminated. The total fill time, t_{fill} , is observed to be approximately 700s. Note that the resin flow between 150 s and 700 s represents significant resin wastage. For the actively controlled case, the error shows a similar profile to the uncontrolled case in early stages of the fill. The actively controlled flow front also first reaches the line vent at $t_{fill}^* = 150$ s; however, the total fill time is reduced to $t_{fill} = 525$ s which represents effectively reduced resin waste.

CONCLUSIONS

An active localized heating based control for the VARTM process was presented where the target positions for heating are determined interactively with the process using feedback of flow

front locations and the heating power is based on maximizing cure subject to the constraint on the maximum cure value. The control logic implemented in conjunction with a physics based process model was used to run parametric studies to demonstrate the viability of the control scheme without leading to premature resin gelation during fill. Practical implementation of the controller in a prototype experimental setup was also demonstrated. Overall, the active control scheme was shown to be capable of reducing fill times and wasted resin as well as increasing flow front uniformity.

ACKNOWLEDGEMENTS

This research was funded in part by the National Science Foundation through Grant No. CTS-9912093 and the Air Force Office of Scientific Research (Grant No. F-49620-01-1-0521). Their support is gratefully acknowledged. The authors also acknowledge Owens Corning for providing gratis the fiberglass preform material used in this study.

REFERENCES

1. R.J. Johnson and R. Pitchumani, "Simulation of Active Flow Control Based on Localized Preform Heating in a VARTM Process", *Composites Part A: Applied Science and Manufacturing*, Vol. 37(10), pp. 1815–1830, 2006.
2. S. Advani, "Flow and Rheology in Polymer Composites Manufacturing", *Elsevier*, New York, 1994.
3. R. Parnas, *Liquid Composite Molding*. Hanser, Munich, 2000.
4. B. Ramakrishnan, L. Zhu and R. Pitchumani, "Curing of Composites Using Internal Resistive Heating", *ASME Journal of Manufacturing Science and Engineering*, Vol. 122(1), pp. 124–131, 2000.
5. C. Han, S. Lee and H. Chin, "Development of a Mathematical Model for the Pultrusion Process," *Polymer Engineering and Science*, Vol. 26, pp. 393–404, 1986.
6. M. Opaliki, J. Kenny, and L. Nicolais, "Cure Kinetics of Neat and Carbon-fiber-reinforced TGDDM/DDS Epoxy Systems," *Journal of Applied Polymer Science*, Vol. 61, pp. 1025–1037.
7. M. Kamal and S. Sourour, "Kinetics and Thermal Characterization of Thermoset Cure," *Polymer Engineering and Science*, Volume 13, pages 59–64, 1973.
8. R.J. Johnson and R. Pitchumani, "Enhancement of Flow in VARTM Using Localized Induction Heating", *Composites Science and Technology*, Vol. 63(15), pp. 2202–2215, 2003.
9. F. Incropera, D. DeWitt, T. Bergman and A. Lavine, *Fundamentals of Heat and Mass Transfer*. Sixth edition, Wiley, New York, 2006.
10. R.J. Johnson and R. Pitchumani, "Active Control of Reactive Resin Flow in a VARTM Process," *Journal of Composite Materials*, Vol. 42(12), pp. 1205–1229, 2008.